Proceedings of the Seventh International Conference on
Railway Technology: Research, Development and Maintenance
Edited by: J. Pombo
Civil-Comp Conferences, Volume 15, Paper 9.5
Civil-Comp Press, Edinburgh, United Kingdom, 2026
ISSN: 2753-3239, doi: 10.4203/ccc.15.9.5

A Roller Rig Evaluation of the Effects of Top-of-Rail Friction Modifiers on Braking Distance and Track Wear

M. Ahmadian[1] and Y. Pan[2]

**[1]Center for Vehicle Systems and Safety, Virginia Tech
Blacksburg, Virginia, USA
[2]Department of Vehicle and Transportation, College of Transportation, Tongji University, China**

Abstract

Top-of-rail friction modifiers (TORFMs) are widely used to manage wheel–rail friction, reduce wear, and maintain an acceptable traction level. However, the relationship between the applied amount of TORFM, traction recovery, and wheel surface wear remains an important practical issue. This study experimentally investigates the influence of TORFM quantity on longitudinal traction behaviour and wheel wear morphology using the VT-FRA roller rig. A biodegradable TORFM is applied to the wheel–rail contact band in light, moderate, and heavy quantities, and the results are compared with an unlubricated baseline. The tests are conducted under controlled conditions with 10.0 kN rig wheel load, 3.0 km/h running speed, 2.0% creepage, zero angle of attack, and zero cant angle. The results show that TORFM significantly delays the recovery of the traction coefficient to the unlubricated steady-state level. The recovery time increases from approximately 7 min under dry contact to 31, 39, and 52 min for the light, moderate, and heavy TORFM conditions, respectively. Normalized traction-duration analysis indicates that the light TORFM application provides the highest material efficiency. Wheel surface measurements obtained using an integrated 3D laser profiler further show that wheel wear becomes deeper and more clearly defined as the TORFM amount decreases. Although the heavy application produces the largest absolute wear reduction, the light application provides the most efficient wear protection per unit amount of TORFM.

Keywords: VT-FRA Roller Rig, Top-of-Rail Friction Modifier (TORFM), wheel wear, rail wear, traction, adhesion, third-body layer.

1 Introduction

Top-of-rail friction modifiers (TORFMs) are widely used as friction management materials at the wheel–rail interface. Unlike conventional lubricants that mainly aim to reduce friction, TORFMs are designed to regulate the interfacial friction within a desirable range so that adequate traction and braking capacity can be maintained while wheel and rail damage are reduced. In practice, TORFMs have been applied in North America, Australia, Europe, and other railway systems to mitigate wheel–rail wear, control curve squeal, reduce lateral forces, and improve operating efficiency. Many commercial TORFMs are water-based suspensions. During wheel–rail contact, the carrier medium evaporates or is expelled, while solid constituents remain in the contact region and interact with the naturally generated third-body layer on the railhead [1–3].

The tribological performance of TORFMs has been studied using different laboratory and field approaches. Li et al. [4] and Arias-Cuevas et al. [5] examined friction modifiers in contaminated and wet wheel–rail contacts using rolling–sliding twin-disc tests, showing that certain solid particles in the modifier can help recover adhesion under low-adhesion conditions. Lewis et al. [6] investigated the influence of environmental conditions using a pin-on-disk apparatus and reported that humidity and temperature can affect the evaporation process and thus the effective duration of the modifier. Galas et al. [7] further studied the role of individual TORFM constituents and highlighted the importance of the base medium and film formation in determining friction behaviour. Buckley-Johnstone et al. [8] compared friction modifier performance at two laboratory test scales and observed reductions in wear severity and subsurface deformation when TORFM was present. These studies have provided important insight into TORFM mechanisms, particularly regarding adhesion recovery, film persistence, and surface protection.

Despite this progress, the practical question of how much TORFM should be applied remains insufficiently resolved. In railway operation, applying too little material may not provide sufficient friction control or wear protection, whereas excessive application may be inefficient and may not fully contribute to the active wheel–rail contact. The amount of TORFM retained within the running band, the time required for adhesion to return to an unlubricated state, and the resulting wear morphology are all important for evaluating application efficiency. Previous laboratory studies have often focused on friction or adhesion evolution, while the detailed surface form of the worn running band has received less attention. However, wear morphology can provide additional evidence of how the contact surface evolves and how the applied TORFM changes the material removal pattern.

This study experimentally investigates the effect of TORFM quantity on longitudinal traction behaviour and wheel surface wear using the VT-FRA roller rig. A biodegradable TORFM commonly used in railway applications is applied to the wheel–rail contact band in different controlled quantities, representing light, moderate, and heavy application conditions. The tests are conducted under the same wheel load, creepage, running speed, angle of attack, and cant angle so that the influence of TORFM amount can be isolated. The longitudinal traction force is recorded during each test, and the wheel surface is measured before and after testing using an integrated 3D laser profiler. In addition to comparing traction recovery and wear reduction, this paper places particular emphasis on the measured wear morphology and average surface profile evolution, providing a more direct view of how TORFM quantity affects the development of the worn running band.

2 Methods

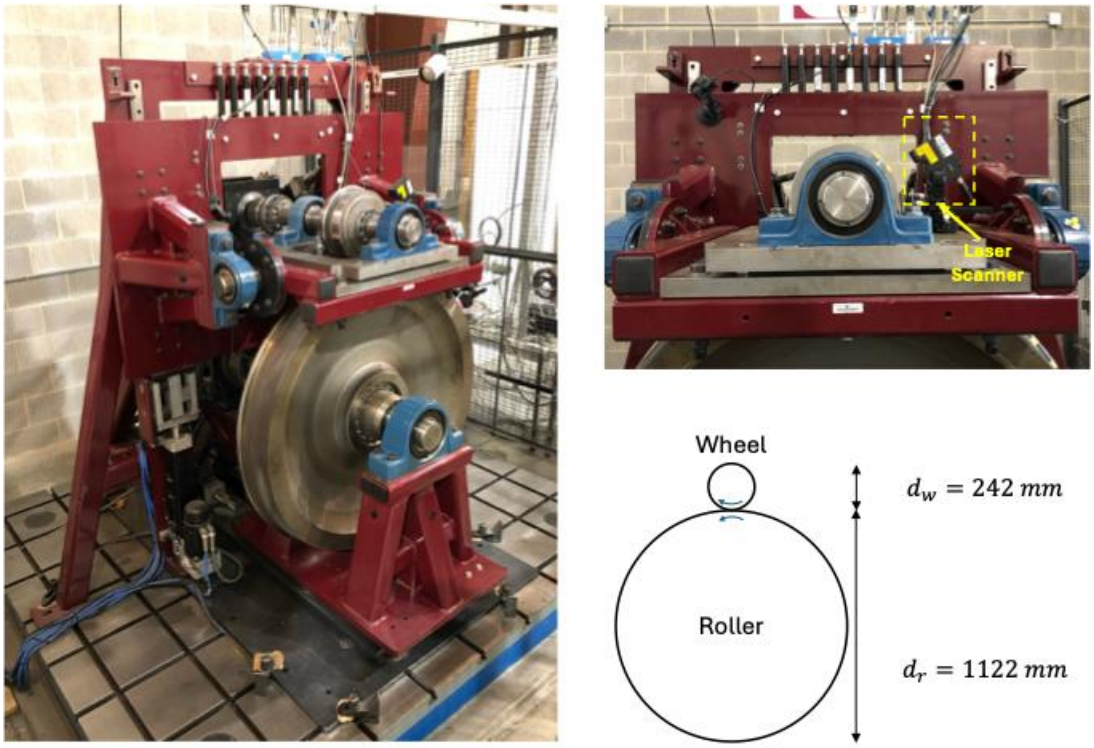

Figure 1: VT-FRA Roller Rig with high-precision laser scanner

Figure 1 shows the VT-FRA roller rig used in this study to reproduce controlled wheel–rail contact conditions in the laboratory. The test rig consists of a scaled wheel running against a large rotating roller, where the roller represents the rail surface. The cylindrical test wheel has a diameter of 242 mm, while the roller diameter is 1122 mm. This large roller-to-wheel diameter ratio helps reduce the geometric distortion of the contact patch and provides a closer representation of wheel–rail rolling contact than conventional small twin-disc arrangements.

The wheel and roller are driven independently by servo motors, allowing the relative rolling speed and creepage to be accurately controlled during testing. The rig is also equipped with loading and positioning systems so that the wheel load, contact location, angle of attack, and cant angle can be adjusted according to the required test condition. In addition to force measurement, a 3D laser scanner is mounted on the rig to capture the wheel surface topography before and after testing. This measurement capability is essential for evaluating both the amount of wheel wear and the detailed morphology of the worn running band under different TORFM application conditions.

Table 1. Test parameter during the experiment

Test Parameter	Value/Description	Test Parameter	Value/Description
Wheel Profile	Cylinder Wheel	Test Speed (km/h)	3.0 km/h
Roller Profile	US-136 Rail	Creepage	2.0%
Rig Wheel Load (kN)	10.0 kN	Angle of Attack (°)	0
Equivalent Field Wheel Load	160.0 kN	Cant Angle (°)	0

Table 1 summarizes the main test parameters used in the experiments. A cylindrical wheel profile and a scaled US-136 rail profile were selected to represent the wheel–rail contact pair in the roller-rig tests. The rig wheel load was set to 10.0 kN, corresponding to an equivalent full-scale wheel load of 160.0 kN. All tests were conducted at a running speed of 3.0 km/h and a creepage of 2.0%. The angle of attack and cant angle were both set to zero so that the influence of TORFM quantity could be examined under a simplified longitudinal rolling contact condition. By keeping these parameters unchanged among the different tests, the observed differences in traction evolution and wheel surface wear can be mainly attributed to the applied TORFM amount.

Figure 2 summarizes the main preparation and testing procedure used in the TORFM experiments. Before each test, the wheel surface was mechanically redressed and cleaned so that the experiment started from a repeatable initial surface condition. The roller speed was then adjusted to establish the zero-creepage condition, which provided the reference for imposing the prescribed 2% creepage during the traction test. A pressure-sensitive film was temporarily placed on the roller surface and brought into contact with the wheel to identify the running band, as shown in Figure 2(a). This step ensured that the TORFM was applied to the actual contact region rather than to an arbitrary location on the roller surface. After the contact band was identified, a syringe with 1.0 cc capacity and 0.02 cc resolution, shown in Figure 2(b), was used to control the applied amount of TORFM. The material was deposited onto the freely rotating roller surface along the measured contact band, as illustrated in Figure 2(c). Different tests were conducted with different application amounts, including light, moderate, and heavy TORFM conditions. The wheel and roller were then brought into rolling contact, and the wheel speed was adjusted relative to the roller speed to generate 2% creepage. During the 60-min test, the longitudinal traction force and wheel load were recorded so that the traction coefficient could be calculated.

After each test, the wheel and roller surfaces were inspected before cleaning to examine the remaining TORFM and third-body material on the running band. Figures 2(d)–2(f) show examples of the post-test contact surfaces with TORFM residue on the wheel and roller. The surfaces were then cleaned to remove the remaining third-body layer, and the wheel surface was measured using the integrated 3D laser profiler. The pre-test and post-test surface measurements were used to evaluate the evolution of the wheel surface profile and to calculate the wheel wear generated during the experiment.

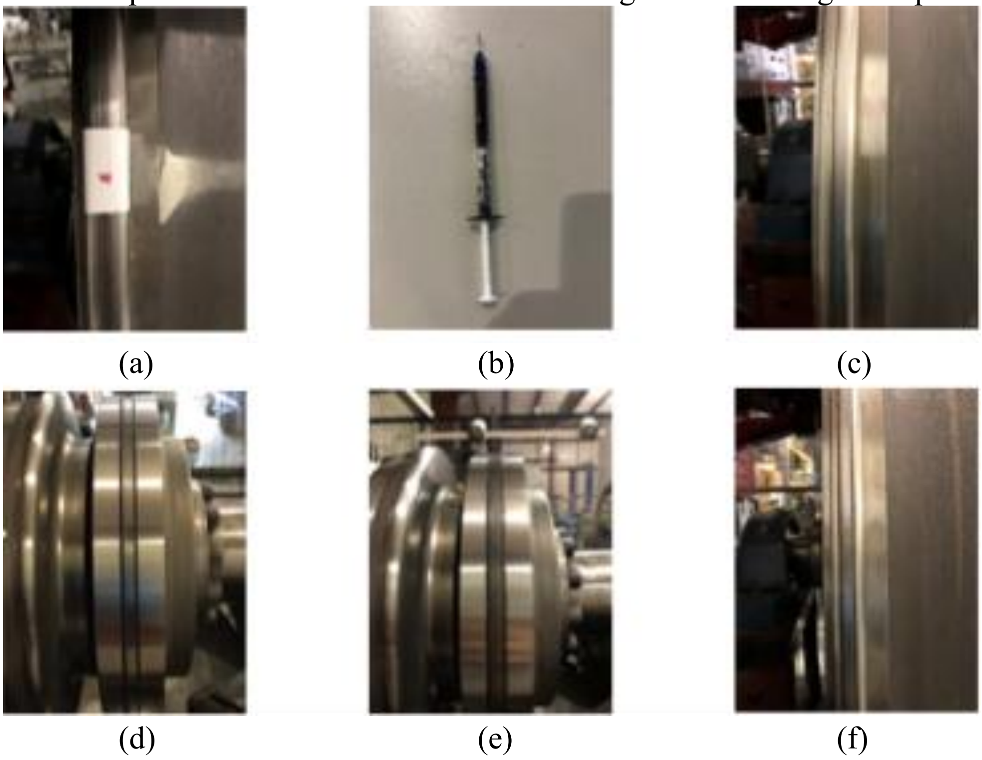

Figure 2: Test preparation and procedure: (a) pressure-sensitive film used to identify the contact band; (b) syringe used for controlled TORFM application; (c) TORFM applied to the roller running band; (d) wheel surface after one test; (e) wheel surface with visible TORFM residue after one test; (f) roller surface with TORFM residue after one test.

3 Results

Figure 3 shows the wheel surface condition before testing and after the 60-min experiments under different TORFM application levels. The wheel was carefully redressed before each test to provide a smooth and repeatable initial surface. After testing, the unlubricated case shows a clearly developed running band, indicating direct material removal under dry wheel–rail contact. When a light amount of TORFM is applied, the running band becomes less severe, and little material accumulation is observed outside the contact region, suggesting that most of the applied TORFM remains within the active contact band during the test. For the moderate and heavy application cases, the worn band is further affected by the presence of TORFM; however, visible residues appear along the edges of the running band, especially under the heavy lubrication condition. This indicates that part of the additional TORFM is squeezed away from the central contact region rather than fully participating in the wheel–rail interaction. Overall, Figure 3 demonstrates that TORFM can mitigate the visible wear band, but increasing the application amount does not necessarily mean that all added material contributes effectively to contact protection.

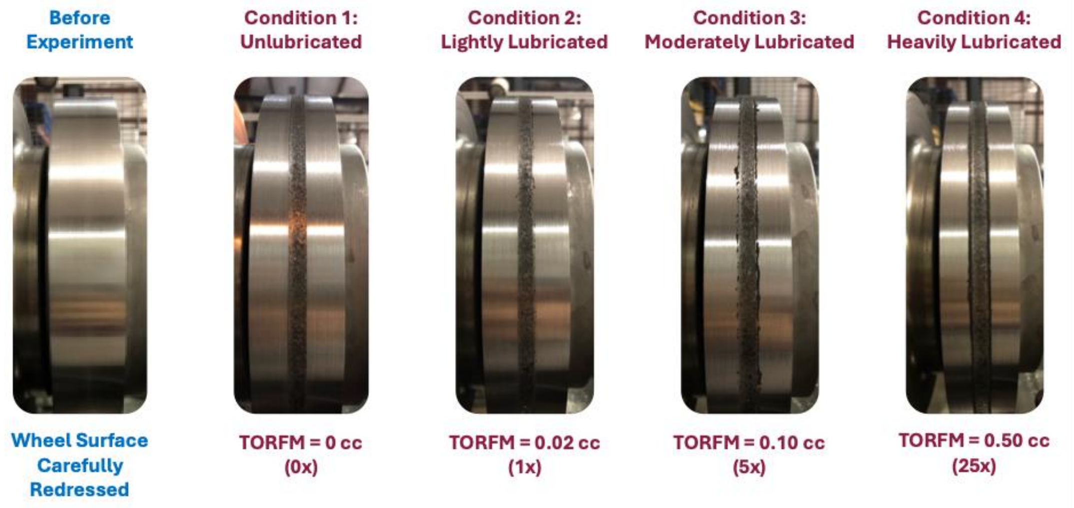

Figure 3: Wheel surface conditions before and after the 60-min experiments for different quantities of TORFM [10]

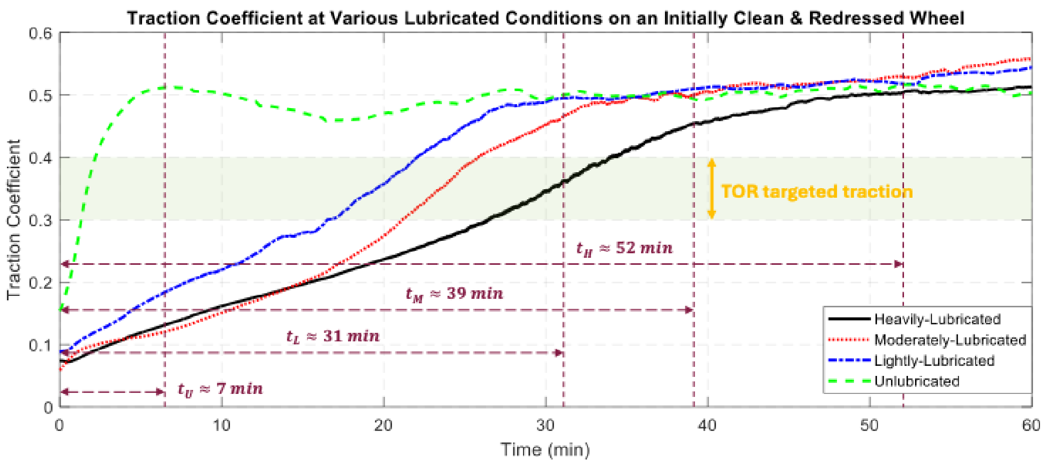

Figure 4: Traction coefficient with different quantities of TORFM []

Figure 4 compares the time histories of the longitudinal traction coefficient for the unlubricated baseline and three TORFM application levels on an initially clean and redressed wheel surface. The traction coefficient is calculated as the longitudinal traction force divided by the applied wheel load. In the unlubricated case, the coefficient increases rapidly at the beginning of the test and reaches approximately 0.5 within the first 7 min. After this initial rise, a temporary reduction is observed, followed by a gradual return to a relatively stable level close to 0.5. This response indicates that, under dry contact, the wheel–rail interface quickly develops a high-adhesion condition after a short running-in period. The TORFM-lubricated cases show a markedly slower transition toward the high-adhesion state. Rather than reaching the steady level within several minutes, the traction coefficient increases progressively over a much longer period. The time required for the coefficient to approach 0.5 is approximately 31 min for the lightly lubricated case, 39 min for the moderately lubricated case, and 52 min for the heavily lubricated case. These durations are about 4.4, 5.6, and 7.4 times that of the unlubricated baseline, respectively. Because the TORFM amount is the primary variable changed among these tests, the delayed recovery of traction suggests that the friction modifier effectively suppresses the rapid development of high traction at the contact interface. However, all lubricated cases eventually converge to a similar steady-state range of approximately 0.5–0.55. This convergence implies that, after sufficient running time, the effective TORFM layer is gradually depleted or removed from the running band, and the contact condition tends to return toward the dry unlubricated state.

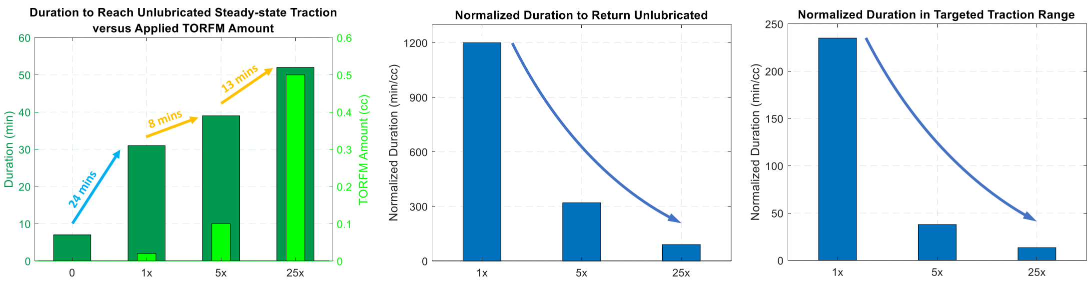

(a) (b) (c)

Figure 5: (a) duration to reach unlubricated steady-state traction; (b) normalized duration to return unlubricated; (c) normalized duration in targeted traction range of [0.3, 0.4]

Figure 5 further quantifies the traction recovery behaviour shown in Figure 4. Figure 5(a) presents the time required for the traction coefficient to recover to the unlubricated steady-state level under different TORFM application amounts. Compared with the dry baseline, the addition of TORFM clearly extends the recovery process. The incremental increases in recovery time between neighbouring conditions are approximately 24 min from the unlubricated case to the light TORFM case, 8 min from the light to moderate TORFM case, and 13 min from the moderate to heavy TORFM case. These increments indicate the additional time delay produced by increasing the TORFM amount at the wheel–rail interface.

To evaluate whether the extra TORFM provides a proportional benefit, the increase in recovery duration is normalized by the corresponding increase in applied TORFM amount, as shown in Figure 5(b). The normalized result shows a strong diminishing-return trend. The light application produces the largest delay per unit TORFM, whereas the moderate and heavy applications provide much smaller additional benefit relative to the extra material added. This suggests that a light TORFM application is more efficient in delaying the return to the unlubricated traction state. In contrast, excessive TORFM application may be inefficient because part of the material is squeezed out of the contact band and accumulates near the band edges rather than actively contributing to traction control.

The TORFM used in this study is intended to maintain the traction coefficient within a target range of approximately 0.3–0.4. Therefore, in addition to the time required to reach the unlubricated steady state, it is also meaningful to examine how long the traction coefficient remains within this preferred range. The shaded region in Figure 4 indicates this target traction interval. Using the same normalization approach, Figure 5(c) compares the normalized duration within the target range for different TORFM quantities. The result again shows that the light TORFM application provides the highest duration per unit material in the target traction range. Increasing the TORFM amount beyond the light application does extend the absolute duration, but the gain is not proportional to the added material. From a material-efficiency perspective, applying more TORFM than needed may therefore offer limited practical advantage.

The integrated 3D laser profiler was used to examine the change in wheel surface topography under different TORFM lubrication conditions. Figure 6 gives an example for the heavily lubricated case. Prior to the test, the wheel surface was scanned over one full revolution while the wheel rotated at a controlled speed, providing the initial surface condition. After the 60-min test, the wheel and roller were cleaned to remove the remaining third-body material, and the wheel surface was scanned again using the same procedure. Figure 6(a) compares the measured two-dimensional surface maps before and after testing. The initial surface is relatively uniform, whereas the post-test surface shows a distinct running band caused by material removal during wheel–rail contact. To further quantify this topographical change, the surface height data were averaged along the circumferential direction at each lateral position, producing the average surface profiles shown in Figure 6(b). The difference between the before-test profile and the after-test profile represents the material loss generated during the experiment. Therefore, the hatched region between the two profiles can be interpreted as the wheel wear accumulated over the test duration.

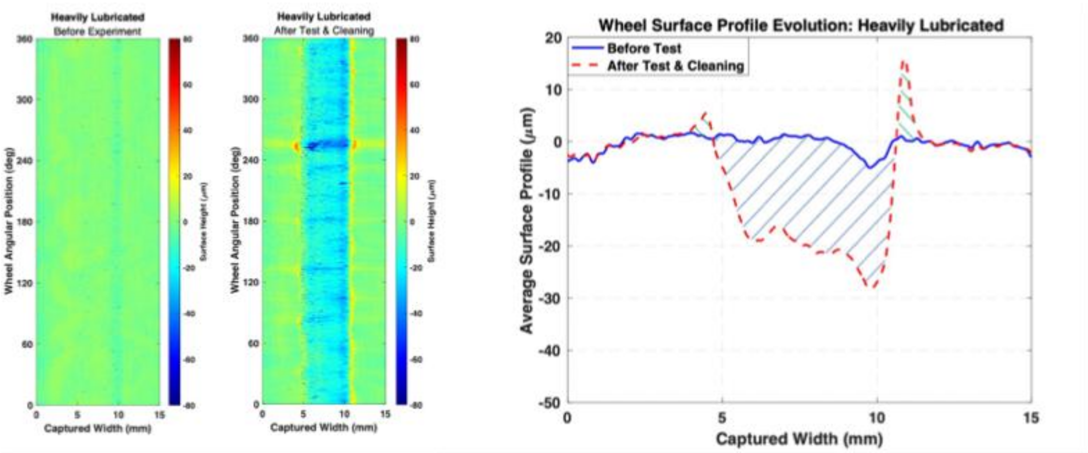

(a) (b)

Figure 6: Sample measurements for lightly-lubricated condition: (a) wheel surface 2D images before the experiment and after the experiment with cleaning; (b) average wheel surface profile evolution

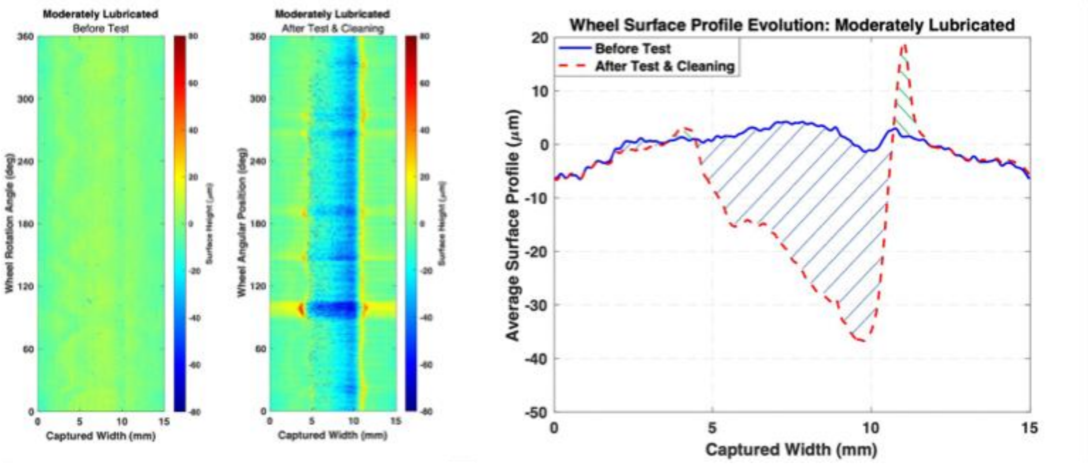

(a) (b)

Figure 7: Sample measurements for moderately-lubricated condition: (a) wheel surface 2D images before the experiment and after the experiment with cleaning; (b) average wheel surface profile evolution

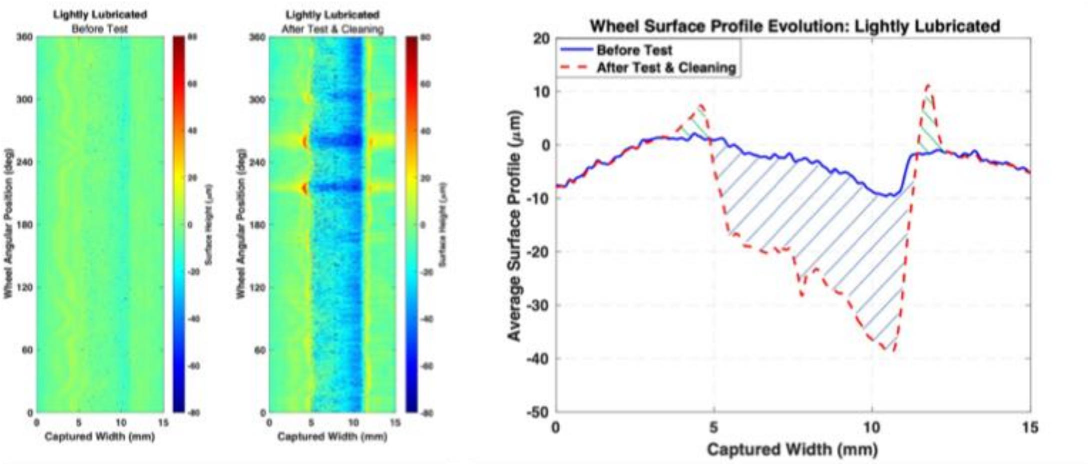

(a) (b)

Figure 8: Sample measurements for lightly-lubricated condition: (a) wheel surface 2D images before the experiment and after the experiment with cleaning; (b) average wheel surface profile evolution

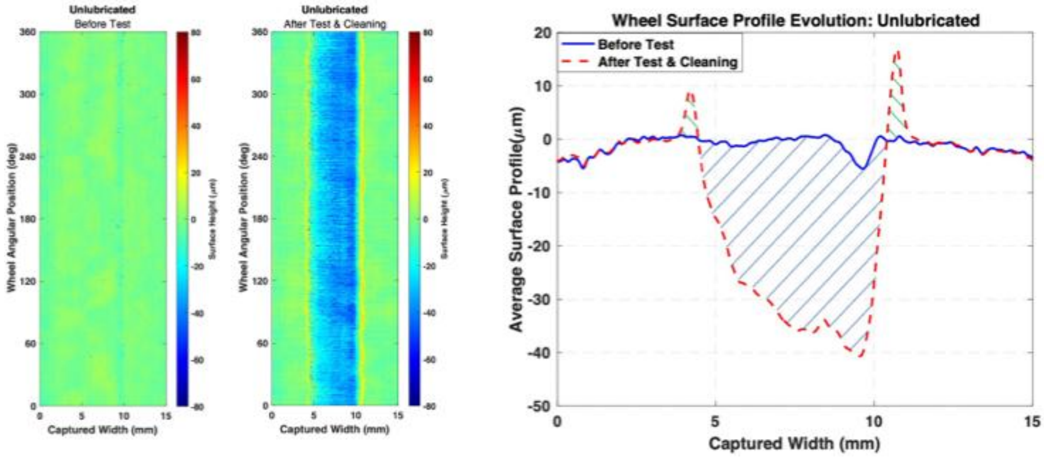

(a) (b)

Figure 9: Sample measurements for a non-lubricated condition: (a) wheel surface 2D images before the experiment and after the experiment with cleaning; (b) average wheel surface profile evolution

Figures 7–9 present the wheel surface measurements and the corresponding profile evolution for the moderately lubricated, lightly lubricated, and unlubricated conditions, respectively. In each figure, the two-dimensional surface maps in part (a) compare the wheel surface before testing and after the test with cleaning, while part (b) shows the averaged surface profile across the running band. A clear trend can be observed when the TORFM amount is reduced. For the moderately lubricated condition in Figure 7, a worn running band is visible after the test, but the depression in the averaged profile remains relatively limited. With the light TORFM application in Figure 8, the worn region becomes more pronounced, and the after-test profile shows a deeper material-loss region over the contact band. The most severe surface change appears in the unlubricated case in Figure 9, where the post-test surface map shows a continuous and distinct wear band, and the averaged profile exhibits the largest downward shift relative to the initial profile. The increasing hatched area from the moderately lubricated case to the unlubricated case indicates that wheel material loss increases as the TORFM amount decreases. These results confirm that TORFM affects not only the overall wear quantity but also the morphology of the worn surface, with insufficient or absent lubrication leading to a deeper and more clearly defined wear scar.

The wear volume for each lubrication condition was determined using the same profile-based calculation method described above. Figure 10(a) compares the percentage reduction in wheel wear relative to the unlubricated case after the 60-min test. The light, moderate, and heavy TORFM applications reduce wheel wear by approximately 16%, 19%, and 39%, respectively, confirming the beneficial role of TORFM in mitigating material loss at the wheel–rail interface. However, the wear reduction does not increase in proportion to the amount of TORFM applied.

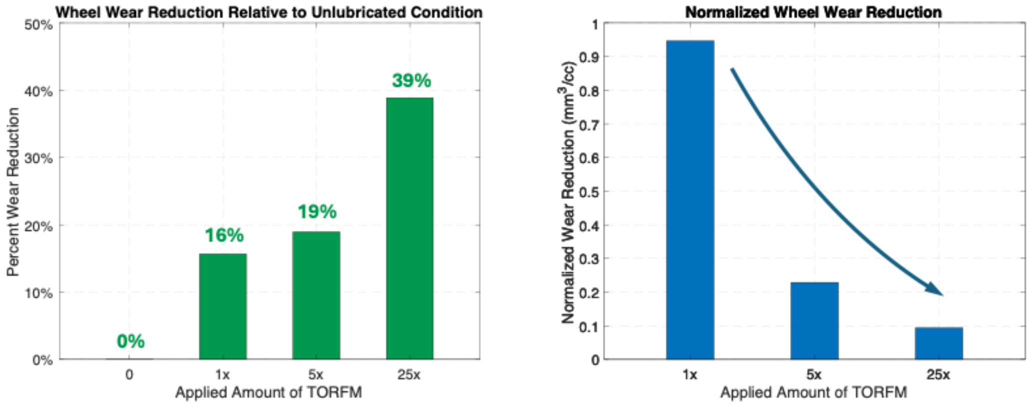

(a) (b)

Figure 10: VT-FRA Roller Rig with high-precision laser scanner [10]

To further assess the material efficiency of different application levels, the wear reduction was normalized by the corresponding TORFM quantity, as shown in Figure 10(b). The normalized result indicates that the light TORFM application provides the highest wear-reduction efficiency per unit amount of material. Although the heavy application produces the largest absolute reduction in wear, its normalized benefit is much lower. This suggests that adding more TORFM beyond a light application does not necessarily lead to a proportionate improvement in wear protection. One possible reason is that, under moderate and heavy lubrication conditions, part of the applied TORFM is squeezed out of the running band and accumulates near the edges of the contact region, reducing the fraction of material that actively participates in wheel–rail contact. It should also be noted that the present wear comparison is based on the final surface condition after a 60-min test. Additional experiments with shorter test durations would be useful for capturing the time-dependent development of wear and for clarifying how the protective effect of TORFM evolves during the early, intermediate, and late stages of contact.

4 Conclusions and Contributions

This paper investigated the effect of TORFM quantity on longitudinal traction behaviour and wheel surface wear using the VT-FRA roller rig. The tests were conducted under controlled wheel–rail contact conditions, with only the applied TORFM amount varied among the lubricated cases.

The results show that TORFM significantly delays the recovery of the traction coefficient to the unlubricated steady-state level. The recovery time increases from approximately 7 min in the unlubricated case to 31, 39, and 52 min for the light, moderate, and heavy TORFM applications, respectively. However, the normalized traction-duration results indicate a clear diminishing-return effect, with the light application providing the highest efficiency per unit amount of TORFM.

The 3D laser surface measurements further show that TORFM changes both the amount and morphology of wheel wear. As the TORFM amount decreases, the worn running band becomes deeper and more clearly defined. Compared with the unlubricated case, the light, moderate, and heavy applications reduce wheel wear by approximately 16%, 19%, and 39%, respectively. Although the heavy application gives the largest absolute wear reduction, the light application provides the best normalized wear-reduction efficiency.

Overall, the findings suggest that a light TORFM application can offer an effective balance between traction control and wear mitigation. Excessive TORFM may provide additional absolute benefit, but the improvement is not proportional to the added material, partly because excess material can be squeezed out of the active contact band.

Acknowledgements

The authors acknowledge the funding support of the Federal Railroad Administration.

References

[1]. Vollebregt, E., Detailed wheel/rail geometry processing with the conformal contact approach. Multibody System Dynamics, 52(2), 135-167, 2021.
[2]. Hardwick, C., Lewis, S., and Lewis, R., The effect of friction modifiers on wheel/rail isolation at low axle loads. Proceedings of the Institution of Mechanical Engineers, Part F: Journal of Rail and Rapid Transit, 228(7), 768-783, 2013.
[3]. Harmon, M., Santa, J. F., Jaramillo, J. A., Toro, A., Beagles, A., and Lewis, R., Evaluation of the coefficient of friction of rail in the field and laboratory using several devices. Tribology - Materials, Surfaces & Interfaces, 14(2), 119-129, 2020.
[4]. Li, Z., Arias-Cuevas, O., Lewis, R., and Gallardo-Hernández, E. A., Rolling–Sliding Laboratory Tests of Friction Modifiers in Leaf Contaminated Wheel–Rail Contacts. Tribology Letters, 33(2), 97, 2008.
[5]. Arias-Cuevas, O., Li, Z., Lewis, R., and Gallardo-Hernández, E. A., Rolling–sliding laboratory tests of friction modifiers in dry and wet wheel–rail contacts. Wear, 268(3), 543-551, 2010.
[6]. Lewis, S. R., Lewis, R., Olofsson, U., Eadie, D. T., Cotter, J., and Lu, X., Effect of humidity, temperature and railhead contamination on the performance of friction modifiers: Pin-on-disk study. Proceedings of the Institution of Mechanical Engineers, Part F: Journal of Rail and Rapid Transit, 227(2), 115-127, 2013.
[7]. Galas, R., Kvarda, D., Omasta, M., Krupka, I., and Hartl, M., The role of constituents contained in water–based friction modifiers for top–of–grail application. Tribology International, 117, 87-97, 2018.
[8].Buckley-Johnstone, L., Harmon, M., Lewis, R., Hardwick, C., and Stock, R., A comparison of friction modifier performance using two laboratory test scales. Proceedings of the Institution of Mechanical Engineers, Part F: Journal of Rail and Rapid Transit, 233(2), 201-210, 2019.
[9] Pan, Y., Radmehr, A., Tajaddini, A., and Ahmadian, M., "An Experimental Study of the Influence of the Amount of Top-of-Rail Friction Modifiers on Traction," Proceedings of the 2021 Joint Rail Conference, JRC2021-58433, 2021.

[10] Pan, Y., Radmehr, A., and Ahmadian, M., “Experimental evaluation of amount and repeated applications of top of rail friction modifiers on wear and adhesion,” International Journal of Rail Transportation, 11(6), 855–871, 2023.